Inorganic Chemistry

Article

pubs.acs.org/IC

Charged, but Found "Not Guilty": Innocence of the Suspect Bridging Ligands $[RO(O)CNNC(O)OR]^{2-} = L^{2-}$ in $[(acac)_2Ru(\mu\text{-}L)Ru(acac)_2]^n$, n = +,0,−,2−

Sayak Roy,[†] Biprajit Sarkar,[†] Hans-Georg Imrich,[†] Jan Fiedler,[‡] Stanislav Záliš,[‡] Reyes Jimenez-Aparicio,[§] Francisco A. Urbanos,[§,⊥] Shaikh M. Mobin,[∥] Goutam Kumar Lahiri,*[,∥] and Wolfgang Kaim*[,†]

[†]Institut für Anorganische Chemie, Universität Stuttgart, Pfaffenwaldring 55, D-70550 Stuttgart, Germany

[‡]J. Heyrovský Institute of Physical Chemistry, v.v.i., Academy of Sciences of the Czech Republic, Dolejškova 3, CZ-18223 Prague, Czech Republic

[§]Departamento de Química Inorgánica, Facultad de Ciencias Químicas, Universidad Complutense, Ciudad Universitaria, E-28040 Madrid, Spain

[∥]Department of Chemistry, Indian Institute of Technology Bombay, Powai, Mumbai-400076, India

Supporting Information

ABSTRACT: Neutral diastereoisomeric diruthenium(III) complexes, *meso*- and *rac*-$[(acac)_2Ru(\mu\text{-adc-OR})Ru(acac)_2]$ ($acac^-$ = 2,4-pentanedionato and adc-OR^{2-} = dialkylazodicarboxylato = $[RO(O)CNNC(O)OR]^{2-}$, R = *tert*-butyl or isopropyl), were obtained from electron transfer reactions between $Ru(acac)_2(CH_3CN)_2$ and azodicarboxylic acid dialkyl esters (adc-OR). The *meso* isomer **3** with R = isopropyl was structurally characterized, revealing two deprotonated and N−N coupled carbamate functions in a reduced dianionic bridge with d_{N-N} = 1.440(5) Å. A rather short distance of 4.764 Å has been determined between the two oxidized, antiferromagnetically coupled Ru^{III} centers. The *rac* isomer **4** with R = isopropyl exhibited stronger antiferromagnetic coupling. While the oxidation of the neutral compounds was fully reversible only for **3** and **4**, two well-separated ($10^8 < K_c < 10^{10}$) reversible one-electron reduction steps produced monoanionic intermediates $\mathbf{1}^-$−$\mathbf{4}^-$ with intense ($\varepsilon \approx 3000\ M^{-1}\ cm^{-1}$), broad ($\Delta\nu_{1/2} \approx 3000\ cm^{-1}$) absorptions in the near-infrared (NIR) region around 2000 nm. The absence of electron paramagnetic resonance (EPR) signals even at 4 K favors the mixed-valent formulation $Ru^{II}(adc\text{-}OR^{2-})Ru^{III}$ with innocently behaving bridging ligands over the radical-bridged alternative $Ru^{II}(adc\text{-}OR^{\bullet-})Ru^{II}$, a view which is supported by the metal-centered spin as calculated by density functional theory (DFT) for the methyl ester model system. The second reduction of the complexes causes the NIR absorption to disappear completely, the EPR silent oxidized forms $\mathbf{3}^+$ and $\mathbf{4}^+$, calculated with asymmetrical spin distribution, do not exhibit near infrared (NIR) activity. The series of azo-bridged diruthenium complex redox systems $[(acac)_2Ru(\mu\text{-adc-R})Ru(acac)_2]^n$ (n = +,0,−,2−), $[(bpy)_2Ru(\mu\text{-adc-R})Ru(bpy)_2]^k$ (k = 4+,3+,2+,0,2−), and $[(acac)_2Ru(\mu\text{-dih-R})Ru(acac)_2]^m$ (m = 2+,+,0,−,2−; dih-R^{2-} = 1,2-diiminoacylhydrazido(2-)) is being compared in terms of electronic structure and identity of the odd-electron intermediates, revealing the dichotomy of innocent vs noninnocent behavior.

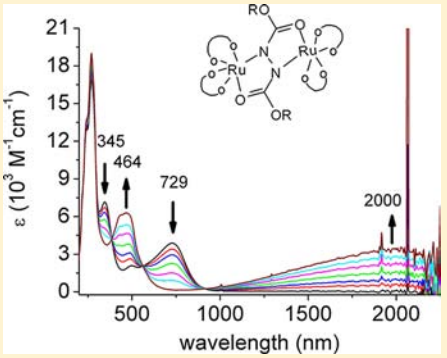

INTRODUCTION

Compounds with strong absorptivity in the near-infrared region (NIR) between 1000 and 2500 nm (10000−4000 cm^{-1}) are sought after materials because of their potential uses in telecommunication and other fields of application.[1] Glass fiber optics technology in particular makes use of bands at 1310 and 1550 cm^{-1} where the radiation losses are minimal.[2] The efficient transmission of information by glass fiber optics was promoted by the discovery of Kao.[3] There are not many classes of reasonably stable compounds studied to this effect.[1] However, a series of investigations[4−6] of complexes such as $[(bpy)_2Ru(\mu\text{-adc-R})Ru(bpy)_2]^k$ ($\mathbf{5}^k$, Scheme 1) as first described by us[7] in terms of unusually strong NIR absorption of the k = 3+ form, has shown activity in terms of optical attenuation around 1550 nm as required for wavelength-division multiplexing and electrochromic activity in the NIR region.[4−6] An additional remarkable feature of these complexes of azodicarboxylic acid derivatives adc-R was the pronounced variability of their electron paramagnetic resonance (EPR)-spectroscopically determined spin distribution between the $Ru^{II}(adc\text{-}R^{2-})Ru^{III}$ (mixed-valency) and the $Ru^{II}(adc\text{-}R^{\bullet-})Ru^{II}$ (radical bridge) alternatives, depending on the donor or acceptor substituents R.[7] Related systems $[(acac)_2Ru(\mu\text{-dih-R})Ru(acac)_2]^m$ ($\mathbf{6}^m$), specifically with m = 1− (dih-R^{2-} = 1,2-diiminoacylhydrazido(2-)) involving all-N donor bridges, have

Received: April 20, 2012
Published: August 21, 2012

   dx.doi.org/10.1021/ic300809w | *Inorg. Chem.* 2012, 51, 9273−9281

Scheme 1. Resonance Structure and Oxidation State Alternatives A or B for Complexes 1^-, 2^-, 3^-, 4^-, 6^- (1e reduced 1−4, 6) and 5^{3+} (1e oxidized $5(PF_6)_2$)

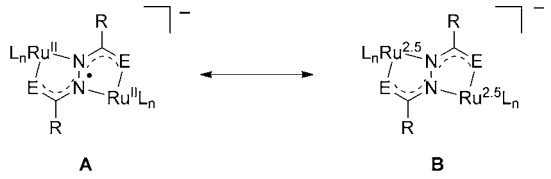

1: L_n = $(acac)_2$, E = O, R = O^{t}Bu (*meso*)
2: L_n = $(acac)_2$, E = O, R = O^{t}Bu (*rac*)
3: L_n = $(acac)_2$, E = O, R = O^{i}Pr (*meso*)
4: L_n = $(acac)_2$, E = O, R = O^{i}Pr (*rac*)
5: L_n = $(bpy)_2$, E = O, R = 1-piperidyl, alkoxyl, CH_3, CF_3, aryl
6: L_n = $(acac)_2$, E = NH, R = aryl

been reported as products of the reductive ring-opening of tetrazines,[8] revealing again intense NIR absorption bands around 1400 nm.

Azodicarboxylic acid derivatives such as the commercially available esters and related systems such as $(dih\text{-}R)^{1-/2-}$ constitute a very special class[9] of redox-active ("noninnocent"[10,11]) ligands because they exhibit the following:

- quinone type two-step redox behavior with a radical intermediate stable against disproportionation,
- a resonance stabilization of the dianionic form,
- a small 6 center π system of which 4 centers can be coordinating,
- a π conjugated bis-chelate function with two [*b*,*b*] edge-sharing[12] five-membered chelate rings (see Scheme 2),

Scheme 2. Bridging Alternatives in a Situation with Two Edge-Sharing Five-Membered Chelate Rings[12]

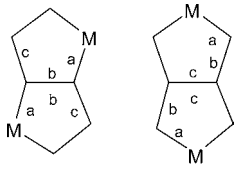

- an "S frame" conformation *s-cis*/E/*s-cis* which allows for a rather short M--M distance (≤5 Å, shorter than in the [*c*,*c*] form, Scheme 2) despite molecule bridging,[7b,12]
- a tuning potential through the substituents R at the non-coordinating carbon π centers (e.g. donor or acceptor substitution),[7a]
- and the possibility to introduce additionally coordinating groups R, leading to bis-tridentate non-innocent ligands.[13]

In organic synthesis the azodicarboxylic acid esters have been widely employed within the Mitsunobu reactions and related conversions.[14]

While structures of two $[(acac)_2Ru(\mu\text{-}dih\text{-}R)Ru(acac)_2]$ systems (R = phenyl, 2-thienyl) have been reported,[8] there is no structure of a neutral (adc-R)-bridged diruthenium complex available. We can present here a first such structure for *meso*-$[(acac)_2Ru(\mu\text{-adc-O}^iPr)Ru(acac)_2]$ and shall describe the formation (Scheme 3), absorption spectroscopy, magnetic resonance, magnetism, (spectro)electrochemistry, and density functional theory (DFT) assessment of the series *meso*- and *rac*-

Scheme 3. Electron Transfer-Accompanied Formation of 1−4

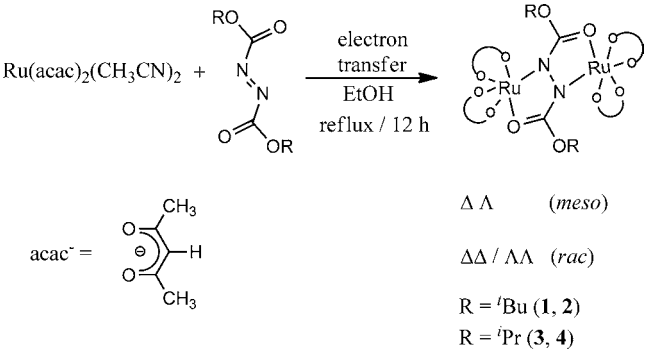

$[(acac)_2Ru(\mu\text{-adc-OR})Ru(acac)_2]^n$ ($\mathbf{1^n}$−$\mathbf{4^n}$, Scheme 1), *n* = +,0,−,2−; R = isopropyl and *tert*-butyl. The presence of two equivalent chiral metal centers in these complexes is responsible for the isomerism.[15]

Renewed interest[16] in redox-noninnocent ("suspect") ligands and their complexes[17] should not distract from the insight that the innocent/noninnocent alternative is an optional behavior of redox-active ligands,[11,17] as will be shown in the following.

EXPERIMENTAL SECTION

The precursor complex $[Ru(acac)_2(CH_3CN)_2]$ was synthesized according to the literature procedure[18] and the ligands di-*tert*-butylazodicarboxylate (adc-O^{t}Bu) and di-*iso*-propylazodicarboxylate (adc-O^{i}Pr) were available commercially from Aldrich.

Instrumentation. Mass spectra were recorded via electrospray ionization (ESI) using a Bruker Daltonics micrOTOF Q instrument. Electron paramagnetic resonance (EPR) spectroscopy in the X band was performed with a Bruker System EMX. UV−vis−NIR absorption spectra were recorded on J&M TIDAS and Shimadzu UV 3101 PC spectrophotometers. Cyclic voltammetry was carried out in 0.1 M Bu_4NPF_6 solutions using a three-electrode configuration (glassy carbon working electrode, Pt counter electrode, Ag wire as pseudoreference) and a PAR 273 potentiostat and function generator. The ferrocene/ferrocenium (Fc/Fc^+) couple served as internal reference. Spectroelectrochemistry was performed using an optically transparent low-temperature cell.[19] A two-electrode capillary served to generate intermediates for X band EPR studies.[20]

Synthesis of [{(acac)$_2$Ru}$_2$(μ-adc-O^{t}Bu)] (1 and 2) and [{(acac)$_2$Ru}$_2$(μ-adc-O^{i}Pr)] (3 and 4). The complexes were synthesized by following a standard procedure, given here for **1** and **2**. An amount of 14 mg (0.062 mmol) of di-*tert*-butylazodicarboxylate was added to the solution of $[Ru(acac)_2(CH_3CN)_2]$ (50 mg, 0.13 mmol) in ethanol and refluxed overnight under aerobic conditions. The solvent was removed under reduced pressure and the remaining solid was purified by chromatography on a neutral Al_2O_3 column. Initially, the red zone containing $Ru(acac)_3$ and the orange zone of $[Ru(acac)_2(CH_3CN)_2]$ were eluted by CH_2Cl_2/hexane (1:4). With CH_2Cl_2/hexane (1:1) a blue solution corresponding to a mixture of **1** and **2** was eluted. The mixture of diastereomers was separated on a preparative TLC plate (silica gel 60 F_{254}) using CH_3CN/CH_2Cl_2 (1:9). While the samples for CHN analysis were used as recrystallized, the materials used for NMR spectroscopy were obtained as powders after prolonged evaporation of solvent of crystallization in vacuo. **1**: Yield: 10 mg (19%); Anal. Calcd. (Found) for **1** × 0.5 CH_3CN, $C_{31}H_{47.5}N_{2.5}O_{12}Ru_2$ (849.36): C, 43.84 (44.09); H, 5.64 (5.93); N, 4.12 (3.81); *m*/*z* = 853.10 (M + Na^+); ^{1}H NMR [$CDCl_3$, δ(ppm)] −10.7 (s, 2H, CH of acac), −6.8 (s, 2H, CH of acac), −6.1 (s, 6H, CH_3 of acac), −4.7 (s, 6H, CH_3 of acac), −0.4 (s, 18H, CH_3 of ^{t}Bu), 2.6 (s, 6H, CH_3 of acac), 3.2 (s, 6H, CH_3 of acac); **2**: Yield: 18 mg (35%); Anal. Calcd. (Found) for $C_{30}H_{46}N_2O_{12}Ru_2$ (826.82): C, 43.47 (43.55); H, 5.59 (5.87); N, 3.38 (3.77); *m*/*z* = 853.10 (M + Na^+); ^{1}H

dx.doi.org/10.1021/ic300809w | *Inorg. Chem.* 2012, 51, 9273−9281

NMR [$CDCl_3$, δ(ppm)] −4.4 (s, 2H, CH of acac), −3.0 (s, 3H, CH_3 of acac), −2.9 (s, 2H, CH of acac), −2.85 (s, 3H, CH_3 of acac), −0.4 (s, 18H, CH_3 of ^{t}Bu), 2.85 (s, 3H, CH_3 of acac), 6.3 (s, 3H, CH_3 of acac). An analogous procedure gave **3** and **4**. Compound **3**: yield: 15 mg (29%). Anal. Calcd. (Found) for **3** × 0.25(CH_3CN;C_6H_{14}), $C_{30}H_{44.25}N_{2.25}O_{12}Ru_2$ (830.61): C, 43.38 (43.15); H, 5.37 (5.55); N, 3.79 (3.77); m/z = 825.70 ($M + Na^+$); ^{1}H NMR[$CDCl_3$, δ(ppm)] −12.5 (s, CH of acac, 2H), −6.75 (s, CH_3 of acac, 6H), −5.69 (s, CH of acac, 2H), −5.17 (s, CH_3 of acac, 6H), −0.62 (m, CH_3 of ^{i}Pr, 12H), 2.51 (s, CH_3 of acac, 6H), 4.30 (s, CH_3 of acac, 6H), 4.52 (sp, CH of ^{i}Pr, 2H). Compound **4**: yield: 12 mg (22%); Anal. Calcd. (Found) for **4** × 0.5 CH_3CN, $C_{29}H_{43.5}N_{2.5}O_{12}Ru_2$ (821.31): C, 42.41 (42.81); H, 5.34 (5.36); N, 4.26 (3.81); m/z = 825.75 ($M + Na^+$); ^{1}H NMR[$CDCl_3$, δ(ppm)] −5.37 (s, CH of acac, 2H), −3.4 (s, CH_3 of acac, 6H), −3.09 (s, CH_3 of acac, 6H), −2.33 (s, CH of acac, 2H), −1.36 (d, CH_3 of ^{i}Pr, 6H), 0.60 (d, CH_3 of ^{i}Pr, 6H), 2.87 (s, CH_3 of acac, 6H), 4.50 (sp, CH of ^{i}Pr, 2H), 7.69 (s, CH_3 of acac, 6H).

Crystal Structure Determination. Single crystals of **3** × H_2O were obtained by slow evaporation of an acetonitrile solution, and the selected single crystal (brown rod, 0.33 × 0.28 × 0.22 mm) was measured on a Nonius Kappa CCD diffractometer using $Mo_{K\alpha}$ radiation (0.71073 Å) at 293 K. The structure was solved and refined by full matrix least-squares on F^2 using SHELX-97 (SHELXTL).[21] All non-hydrogen atoms were refined anisotropically, hydrogen atoms were introduced at the appropriate calculated positions. The water molecule is associated with one of the O atoms of an $acac^-$ ligand (O5·····(H)O111 2.870 Å).

Magnetic Susceptibility Measurements. Variable-temperature magnetic susceptibilities were measured for polycrystalline samples with a Quantum Design MPMS*XL* SQUID (Superconducting Quantum Interference Device) susceptometer over a temperature range of 2 to 300 K at a constant field of 0.1 and 1 T. Each raw data set was corrected for the diamagnetic contributions of both the sample holder and the complex to the susceptibility. The molar diamagnetic corrections were calculated on the basis of Pascal constants. Magnetization measurements were carried out at 2 and 300 K from 0 to 5 T, including also hysteresis loops between −5 and 5 T at the same temperatures. The zero-field-cooled (ZFC) and field-cooled (FC) susceptibility were measured in a magnetic field of 0.1 T from 2 to 300 K. The fitting of the experimental data was carried out using the MATLAB V.5.1.0.421 program.

DFT Calculations. To simplify calculations the ^{i}Pr groups in **3** were replaced by methyl groups. The electronic structure of *meso*-[$(acac)_2$Ru(μ-adc-OMe)Ru$(acac)_2$] was calculated by DFT methods using the Gaussian 09[22] and ADF2010.01[23] program packages. The calculations of the vibrational frequencies were performed at optimized geometries.

The hybrid functional of Perdew, Burke, and Ernzerhof[24] (PBE0) was used within Gaussian (G09/PBE0) together with 6-311G(d) polarized valence triple-ζ basis sets[25] for C, N, and O atoms, 6-31G(d) polarized valence double-ζ basis[26] for H and effective core pseudopotentials and corresponding optimized sets of basis functions[27] with additional f- and g-type polarization functions for Ru.[28] Open shell systems were calculated within spin-unrestricted Kohn−Sham (UKS) formalism. For analysis of singlet diradicals, a symmetry breaking approach (SB-UKS)[29,30] within DFT should be used. Therefore, the calculations on ground-state singlet states were performed using either spin-restricted (RKS) or spin-unrestricted approach. Calculations were performed without any symmetry constraints.

Slater type orbital (STO) basis sets of triple-ζ quality with two polarization functions for the Ru atom and of triple-ζ quality with one polarization function for the remaining atoms were employed within ADF. The inner shells were represented by the frozen core approximation (1s for C, N, O, 1s-3d for Ru were kept frozen). The calculations were done with the functional including Becke's gradient correction[31] to the local exchange expression in conjunction with Perdew's gradient correction[32] to the local correlation (ADF/BP). The scalar relativistic (SR) zero order regular approximation (ZORA) was used within ADF calculations.

RESULTS AND DISCUSSION

Synthesis and Characterization (NMR). The complexes **1**−**4** were obtained by reacting the corresponding azodicarboxylic esters with $Ru(acac)_2(CH_3CN)_2$ under double metal-to-ligand electron transfer and subsequent chromatographic separation of the diastereoisomers which result from the presence of two chiral centers.[15] As the structure determination of a monohydrate (vide infra) demonstrates, the compounds tend to crystallize with small molecules. As a result the elemental analyses fitting required partial inclusion of solvents of crystallization (Exp. Section). In the case of **3** × H_2O the crystal structure was available as evidence.

^{1}H NMR Spectroscopy of the materials indicated paramagnetism through large shifts and some broadening of the signals from the $acac^-$ coligands (see Exp. Section), pointing already to a ruthenium(III) formulation following electron transfer between the electron-rich precursor complex (Ru^{II}) and the strong acceptor ligands adc-OR.[9] The pronounced paramagnetic shift for the $acac^-$ ligands confirms the previously noted[33] interaction between Ru^{III} and such ligands. Since the isopropylester complex **3** could be identified crystallographically as the *meso* form (see below) and **4** accordingly as the *rac* analogue, the ^{1}H NMR spectroscopic distinction between *meso* and *rac* diastereoisomers such as the more high-field shifted CH(acac) and CH_3(acac) resonances for the *meso* alternative were used to assign **1** as the *meso* and **2** as the *rac* isomer for the *tert*-butyl ester pair.

Structure. A single crystal structure analysis was possible for hydrated compound **3**; the results are summarized in Tables 1 and 2, where the experimental data are compared with calculated values as discussed below. Figure 1 shows the molecular structure; the water molecule is weakly hydrogen bonded to one of the O($acac^-$) atoms (O(H)····O 2.870 Å).

Table 1. Selected Crystallographic Parameters of 3×H_2O

empirical formula	$C_{28}H_{42}N_2O_{13}Ru_2$
formula mass	816.79
crystal system	triclinic
space group	$P\bar{1}$
a/Å	8.3121(4)
b/Å	10.9994(6)
c/Å	11.3339(5)
α/deg	118.523(3)
β/deg	106.467(3)
γ /deg	94.777(3)
V/Å^3	843.21(7)
Z	1
μ/mm^{-1}	0.959
T/K	293(2)
D_{calcd}/g cm^{-3}	1.608
F/000	416
θ range/deg	3.72 to 27.50
data/restraints/parameters	3832/0/214
R1, wR2 [$I > 2\sigma(I)$)]	0.0374, 0.0932
R1, wR2 (all data)	0.0467, 0.0999
GoF	1.093
largest diff. peak/hole/e Å^{-3}	0.819, −1.034

The structure analysis of **3** reveals the *meso* configuration in the expected setting with the ligand bridge in "S" conformation,[9] forming two [*b*,*b*] edge-sharing five-membered chelate rings (Scheme 2) with a rather short (nonbonding)

dx.doi.org/10.1021/ic300809w | Inorg. Chem. 2012, 51, 9273−9281

Table 2. Comparison of Selected Bond Lengths (Å) of *meso*-[(acac)$_2$Ru(μ-adc-OR)Ru(acac)$_2$] with G09/PBE0 in Vacuo Calculated Symmetry Averaged Values

	exp.[a]	calc.[b] ^{3}A	calc.[b] ^{1}A (SB-UKS)	calc.[b] ^{1}A RKS
Ru–N1	1.984(3)	1.993	1.991	1.961
Ru–O1	1.993(2)	1.985	1.985	1.995
Ru–O2	2.016(2)	2.008	2.008	2.001
Ru–O4	2.021(2)	2.012	2.013	2.023
Ru–O5	2.011(3)	2.009	2.008	2.027
Ru–O6	2.063(2)	2.062	2.064	2.061
N1–N1_2	1.440(5)	1.415	1.413	1.363
N1_2-C11	1.338(4)	1.327	1.327	1.366
C11–O6	1.263(4)	1.259	1.259	1.243
C2–O1	1.285(4)	1.276	1.276	1.266
C4–O2	1.268(4)	1.264	1.264	1.271
C7–O4	1.274(4)	1.272	1.272	1.264
C9–O5	1.285(5)	1.270	1.270	1.275

[a]R = ^{i}Pr. [b]R = Me.

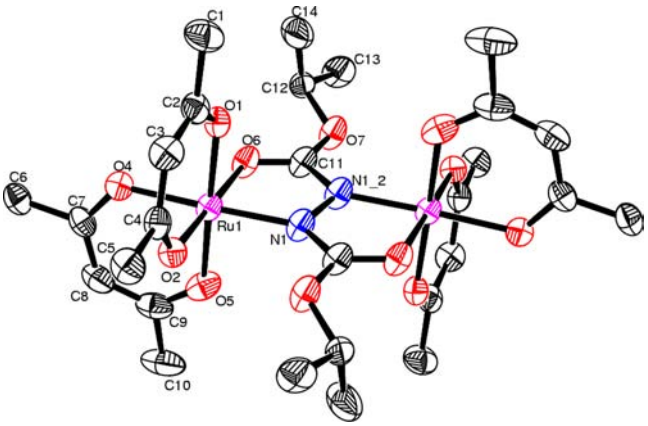

Figure 1. Molecular structure of **3** × H_2O. Thermal ellipsoids at 50% level; hydrogen atoms and solvent water are removed for clarity. The molecule has a crystallographical center of symmetry. Selected bond lengths (Å): Ru1–O6 1.993(2); Ru1–N1 1.984(3); Ru1–O5 2.011(3); Ru1–O2 2.016(2); Ru1–O4 2.021(2); Ru1–O1 2.063(2); N1–N1_2 1.440(5); N1_2-C11 1.338(4); C11–O6 1.263(4); C2–O1 1.285(4); C4–O2 1.268(4); C7–O4 1.274(4); C9–O5 1.285(5).

metal–metal distance of 4.764 Å, despite the separation by a molecular bridge. The central torsional angle of 180° illustrates the planarity of that arrangement, and the short Ru–Ru distance in comparison to the 5.029 Å reported for a related diruthenium(II) bridged compound[7b] confirms the higher oxidation state in **3**. The most revealing bond parameter is the N–N distance of 1.440(5) Å which signifies a single bond[7–9,34,35] and thus the complete two-electron reduction of the azo precursor ligand. An obviously two-electron reduced azodicarboxylic ester **I** has been described as a side-on bonded species relative to (phen)Pd^{II} with d(N–N) = 1.404(5) Å,[36] and the planar diformylhydrazine has d(N–N) = 1.392 (7) Å.[37] The dication in [(bpy)$_2$Ru^{II}(μ-adc-CF$_3$)Ru^{II}(bpy)$_2$](PF$_6$)$_2$ (**5**) was shown to have d(N–N) = 1.463(5) Å.[7b] The bond parameters at the carbaminate carbon atoms C11 in the structure of **I** show a resonance situation with a relatively short C=O bond of 1.263(4) Å and a typical "peptide"-type C11–N1 bond of 1.338(4) Å;[38] the ester bond to O^{i}Pr is also shortened to 1.333(4) Å.

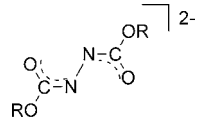

I

The metal coordination is unsymmetrical with one longer, weaker Ru–O6 bond at 2.063(2) Å and a stronger, shorter Ru–N1 bond at 1.984(3) Å to the hydrazido N. The all-N analogue [(acac)$_2$Ru(μ-dih-Ph)Ru(acac)$_2$] (**6**) exhibits a slightly longer Ru–N$_{hydrazido}$ bond of 2.012(4) Å but a rather short Ru–N$_{imine}$ bond of 1.927(5) Å.[8] However, in [(bpy)$_2$Ru^{II}(μ-adc-CF$_3$)Ru^{II}(bpy)$_2$](PF$_6$)$_2$ (**5**) the difference is reversed with a Ru–O distance of 2.093(3) Å but a still longer Ru–N$_{hydrazido}$ bond of 2.151(4) Å, a consequence of the metal donor character in Ru^{II}-containing **5**.[7b]

In conjunction with a somewhat shorter central N–N bond at 1.407(8) Å[8] the observations for **3** suggest a higher extent of bond equilibration and electron delocalization in the case of **6**. Furthermore, the Ru–O$_{acac}$ bonds are shorter for **3** than for **6** which suggests a higher effective oxidation level for the metal in the case **3** presented here. Concluding the structure discussion, the results for **3** are compatible with a 2e-reduced adc-OR bridge and therefore with the evidence for metal-centered magnetism with two exchange-coupled Ru^{III} ions as elaborated in the following.

Magnetism. The temperature dependence of the magnetic susceptibility of structurally characterized **3** has been measured at 0.1 and 1 T between 300 and 2 K. In both cases, the magnetic susceptibility increases with decreasing temperature. However, the susceptibility values vary with the magnetic field, and the variation of the magnetic moment is even more pronounced (Figure 2). The magnetic moments at room

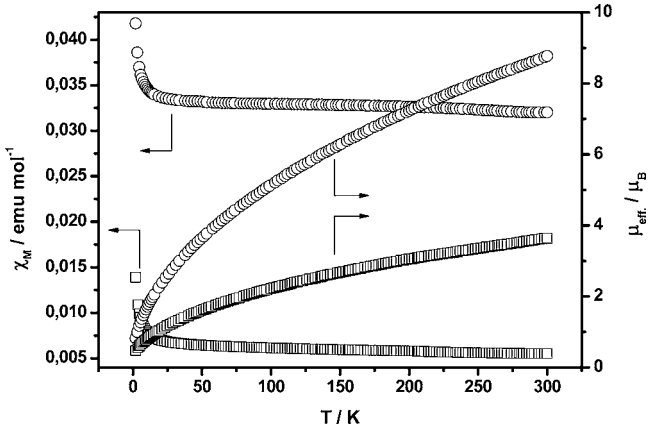

Figure 2. Temperature dependence of the molar magnetic susceptibility and magnetic moment for complex **3** under magnetic fields of 0.1 (○) and 1(□) T, respectively.

temperature are 8.77 and 3.64 μ_B at 0.1 and 1 T, respectively. In both measurements, the magnetic moments decrease with temperature to converge near 0.5 μ_B. This magnetic moment at 2 K could be explained by a strong antiferromagnetic coupling between the two Ru^{III} centers, leading to an almost diamagnetic species at very low temperature.

The field dependence of the magnetic susceptibility and the magnetic moment clearly indicate the presence of ferromagnetism in this compound, even at room temperature. To confirm the presence of ferromagnetic interactions we have carried out measurements of the magnetization versus magnetic

dx.doi.org/10.1021/ic300809w | Inorg. Chem. 2012, 51, 9273–9281

field at 300 and 2 K. At both temperatures **3** shows small hysteresis cycles (Supporting Information, Figure S1) with a coercitivity field of 60 and 100 G and remnant magnetization of 4 and 6 emu mol^{-1} at 300 and 2 K, respectively. These measurements also indicate that the magnetization is saturated at 300 K, with very low spin values, whereas the curve at 2 K does not reach saturation (Supporting Information, Figure S2). This behavior indicates the presence of ferromagnetic interactions over the whole range of temperature studied. However, the ferromagnetism is accompanied by a predominant antiferromagnetic interaction responsible for the drop of the magnetic moment with the temperature and also for the low magnetization value at room temperature.

The zero field cooled (ZFC) and field cooled (FC) thermomagnetization curves at low magnetic field (0.1 T) exhibit a small irreversibility from 300 K, which also confirms the existence of ferromagnetic order just below this temperature (Supporting Information, Figure S3).

The magnetic behavior of the *rac* isomer **4** also shows field dependence of the magnetization, and the curves at 2 and 300 K display a similar shape as those observed for **3** (Supporting Information, Figure S4). The magnetic susceptibility dependence on temperature at 1 T (Supporting Information, Figure S5) shows a slight decrease from 300 to about 75 K and then increases rapidly until 2 K. The magnetic moment of **4** displays a continuous decrease with the temperature suggesting the presence of an antiferromagnetic interaction. In addition, the slight decrease of the susceptibility from 300 to 100 K supports the existence of a strong antiferromagnetic coupling.

The magnetic data of **3** and **4** reveal that these complexes display similar magnetic behavior with a weak ferromagnetism from room temperature to 2 K and a predominant antiferromagnetism in the whole temperature range. However, there are some quantitative differences in the magnetic behavior of these compounds. For example, for **3** the magnetization at 300 K is saturated (Supporting Information, Figure S2) whereas for **4** the saturation is not reached (Supporting Information, Figure S4). In addition, at 1 T the magnetic moments vary from 3.64 to 0.47 μ_B and from 1.96 to 0.32 μ_B for **3** and **4**, respectively. These values suggest that **4** has a stronger antiferromagnetic coupling than **3**.

The strong antiferromagnetic coupling is most likely due to the intramolecular interaction of the spins of Ru^{III} (S = 1/2).[33,39] To support this hypothesis, a DFT analysis was performed for the methyl ester model system *meso*-[$(acac)_2$Ru(μ-adc-OMe)Ru$(acac)_2$]. Geometry optimizations (Table 2) show the configuration with spin density of 0.85 on each ruthenium center as the lowest energy states, either ^{3}A or ^{1}A, with parallel or antiparallel spins, respectively, on the Ru^{III} centers of *meso*-[$(acac)_2$Ru(μ-adc-OMe)Ru$(acac)_2$]. The singlet state with spin density delocalized over the adc-OR bridging ligand is higher in energy by about 0.85 eV. The free energy difference between ferromagnetic and antiferromagnetic states is about 0.003 eV. Table 2 shows that the calculations for both the ^{3}A and ^{1}A states with Ru localized spin describe the experimental geometry of **3** fairly well.

Figure 3 illustrates that the DFT calculated spin density in the triplet state of *meso*-[$(acac)_2$Ru(μ-adc-OMe)Ru$(acac)_2$] is mainly localized on the metal centers, with some contributions from the ligands. The G09/PBE0 calculations yield spin densities of 0.85, 0.18, and 0.03 for each Ru, adc-OMe, and acac, respectively. Supporting Information, Figure S6 shows antiparallel spins on the Ru centers in the case of the ^{1}A state.

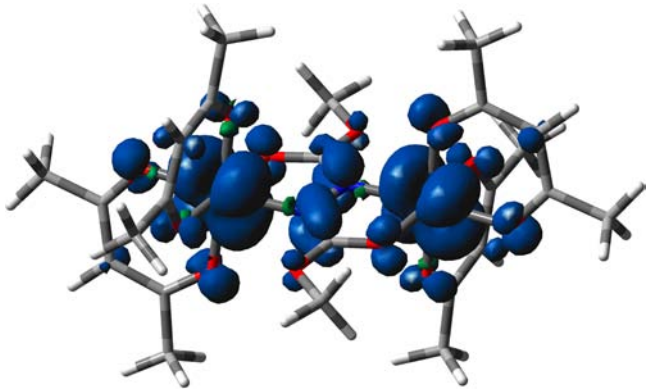

Figure 3. DFT calculated spin densities in the ^{3}A state of *meso*-[$(acac)_2$Ru(μ-adc-OMe)Ru$(acac)_2$]. Blue areas indicate positive and green areas negative spin densities.

In accordance with this DFT study the two S = 1/2 spins are not independent because the orientation of one of them determines the orientation of the other one, leading to an S = 0 or S = 1 state. The presence of a diamagnetic ground S = 0 state with a thermally accessible low-lying excited S = 1 term (the energy difference between them is about 0.003 eV) explain well the magnetic behavior of compound **3**. Thus, the low magnetization values at very low temperatures are in accordance with the preponderance of the S = 0 ground state which leads to a very low magnetic moment. The increase of the temperature produces a higher population of the triplet state, S = 1, leading to an increase of the magnetization from 2 to 300 K. The clear ferromagnetic behavior of complexes **3** and **4** should be a consequence of the alignment of the partially occupied S = 1 spins, probably due to a spin-canting phenomenon. Thus, two opposite phenomena can explain the variation of the ferromagnetism observed from 2 to 300 K. On the one hand, the ferromagnetism increases with decreasing temperature because of the higher alignment of the spins. On the other hand, the increase of the temperature produces a higher population of the ferromagnetic S = 1 term which leads to an increase of the ferromagnetic response. In consequence the hysteresis loops observed at 2 and 300 K are similar (Supporting Information, Figure S1). However, the energy gap between the ground (S = 0) and the excited (S = 1) states in the compounds **3** and **4** may not be identical, leading to different population of these levels. This would explain the observed differences in their magnetic properties. Slight variations in the electronic distribution in each diastereoisomer (revealed also by their NMR spectra) and the foreseeable different packing of the molecules in the solid state will be further responsible for these differences.

The ferromagnetic behavior observed for **3** and **4** would also be compatible with the presence of a small quantity of a ferromagnetic impurity, although the explanation based on the DFT studies is more probable. In addition, the magnetic behavior of **3** and **4** is similar to that observed previously for mononuclear ruthenium complexes interacting with potential radical ligands.[40]

The presence of ferromagnetism from 2 K to room temperature results in the nonlinearity of the magnetization versus the magnetic field, which prevented us to apply the usual approximations to fit the magnetic data of these complexes.

Summarizing, the magnetic data indicate that the decrease of the magnetic moment with the temperature is superimposed by

dx.doi.org/10.1021/ic300809w | *Inorg. Chem.* 2012, 51, 9273−9281

a weak ferromagnetic interaction arising from the presence of a ferromagnetic term ^{3}A with a similar energy as the antiferromagnetic ground term. The variable temperature susceptibility measurements illustrate greater population of the $S = 0$ state for the *rac* isomer **4** in comparison to the *meso* form **3**, but in both cases a weaker intermolecular ferromagnetic interaction, presumably originating from spin canting, is dominated by a strong intramolecular antiferromagnetic coupling.

Cyclic Voltammetry. The compounds **1**−**4** undergo two one-electron oxidation and two one-electron reduction processes. While the *tert*-butyl ester complexes **1** and **2** are only partially reversibly oxidized (Table 3), presumably because of steric interference involving the bulky alkyl groups, the isopropyl analogues **3** and **4** show a reversible first oxidation and two reversible reduction waves in CH_3CN (Figure 4). The second oxidation is irreversible in all cases.

Table 3. Redox Potentials from Cyclic Voltammetry[a]

	E°/V (ΔE_p/mV)			
compound	E_{Ox2}	E_{Ox1}	E_{Red1}	E_{Red2}
1	0.68 (E_{pa})	0.23 (90)[b]	−1.19 (100)	−1.78 (130)
2	0.60 (E_{pa})	0.10 (90)[b]	−1.17 (80)	−1.70 (100)
3	0.94 (E_{pa})	0.13 (90)	−1.13 (70)	−1.62 (80)
4	0.94 (E_{pa})	0.15 (90)	−1.15 (70)	−1.65 (80)

[a] In 0.1 M Bu_4NPF_6/CH_3CN at RT; E_{pa} = anodic peak potential corresponding to irreversible steps. [b] $i_{pc}/i_{pa} < 1$ due to lability of the oxidation product.

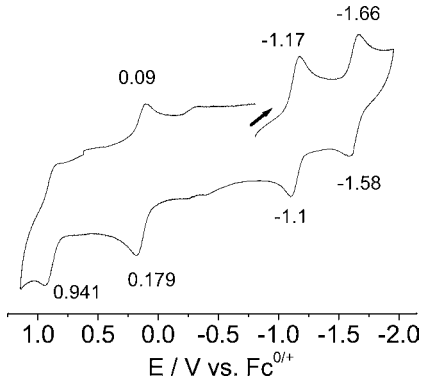

Figure 4. Cyclic voltammogram of **3** in CH_3CN/0.1 M Bu_4NPF_6 at 298 K. The small steps at −0.3 V result from disintegration on oxidation.

The comproportionation constants $K_c = 10^{\Delta E/59\ mV}$ for the monoanions are in a slightly higher range (10^8−10^{10}) than those of the complexes $\mathbf{5}^{3+}$ ($K_c \approx 10^7$) [7] or of the Creutz-Taube ion, $[(H_3N)_5NRu(\mu\text{-pyrazine})Ru(NH_3)_5]^{5+}$ ($K_c \approx 10^6$−10^7)[41] Although the rather high values of comproportionation constants seem to indicate an electronic communication of equivalent metal centers via the bridging ligand, these values alone do not allow for a quantitative assessment of the degree of valence delocalization.[41b,c]

EPR Spectroscopy. EPR studies of the compounds **1**−**4** and of their electrogenerated anions ($\mathbf{1}^-$−$\mathbf{4}^-$) or cations ($\mathbf{3}^+$, $\mathbf{4}^+$) did not produce identifiable signals, even at 4 K. This absence of a direct EPR response for the neutral forms can be attributed to the presence of persistent ferromagnetic interactions[40] as inferred from the above magnetic studies for the neutral compounds **3** and **4**. Another reason for rapid relaxation can be close lying states with significant orbital angular momentum. Spin−orbit coupling as an efficient energy transfer mechanism is also held responsible for the rapid relaxation[42] and thus severe EPR line-broadening as has been observed before for mixed-valent complexes $\mathbf{5}^{3+}$[7] and for the EPR silence of corresponding diosmium analogues.[43] The results therefore suggest dominant metal contributions to the singly occupied MO of the thus $Ru^{III}Ru^{II}$ mixed-valent anions $\mathbf{1}^-$−$\mathbf{4}^-$, as confirmed also by DFT calculations. DFT calculations of the methyl ester model (Supporting Information, Table S1) produced asymmetrical solutions for both the monoanion and the monocation (Supporting Information, Figure S7). Calculated spin densities on the Ru centers are 0.73 and 0.038 or 0.89 and −0.14 for the anion and cation species, respectively. The spin densities on the adc-OMe bridge were calculated at 0.04 and 0.17 in the case of anion and cation, respectively. Clearly, the anions with virtually unchanged N−N bond length relative to the $Ru^{III}(adc\text{-}OR^{2-})Ru^{III}$ precursors (Supporting Information, Table S1) represent hydrazido-bridged mixed-valent species $Ru^{II}(adc\text{-}OR^{2-})Ru^{III}$ with the spin concentrated on Ru2 (Supporting Information, Figure S7). The cationic state is calculated with a very short Ru2−N distance of 1.904 Å (Supporting Information, Table S1) which points to a Ru^{IV} oxidation state and pronounced asymmetry. The other metal center, Ru1, exhibits the features of trivalent ruthenium, and the spin distribution confirms this (Supporting Information, Figure S7). While the calculated spin density of 0.17 and the slightly shortened N−N bond of the bridging ligand suggest more orbital mixing in the cation than in the anion, the most appropriate formulation is $Ru^{III}(adc\text{-}OR^{2-})$-$Ru^{IV}$ and not a 3-spin coupled[44] situation $Ru^{III}(\mu\text{-}adc\text{-}O^iPr^{\bullet-})Ru^{III}$. Both the anion and cation were found EPR silent even at very low temperatures, a not uncommon situation for diruthenium mixed-valent species.[7,42]

From these results we assign the oxidation state combinations to the members of the redox series shown in Scheme 4.

UV−vis−NIR Spectroelectrochemistry. The reversibility of the first one-electron oxidation process for **3** and **4** and of the two successive reductions of all four compounds allowed us to perform corresponding UV−vis−NIR spectroelectrochemical experiments in an OTTLE cell (Figure 5). The observation of isosbestic points and the near 100% regeneration of the

Scheme 4. Oxidation State Assignments for the Redox Series

$$[(acac)_2Ru^{III}(adc\text{-}OR^{2-})Ru^{IV}(acac)_2]^+$$

$$\overset{-\,e^-}{\rightleftharpoons}\ \overset{+\,e^-}{}$$

$$[(acac)_2Ru^{III}(adc\text{-}OR^{2-})Ru^{III}(acac)_2]$$

$$\overset{-\,e^-}{\rightleftharpoons}\ \overset{+\,e^-}{}$$

$$[(acac)_2Ru^{III}(adc\text{-}OR^{2-})Ru^{II}(acac)_2]^-$$

$$\overset{-\,e^-}{\rightleftharpoons}\ \overset{+\,e^-}{}$$

$$[(acac)_2Ru^{II}(adc\text{-}OR^{2-})Ru^{II}(acac)_2]^{2-}$$

dx.doi.org/10.1021/ic300809w | Inorg. Chem. 2012, 51, 9273−9281

starting spectra on reverse electrolysis confirm the reversibility as noted from cyclic voltammetry.

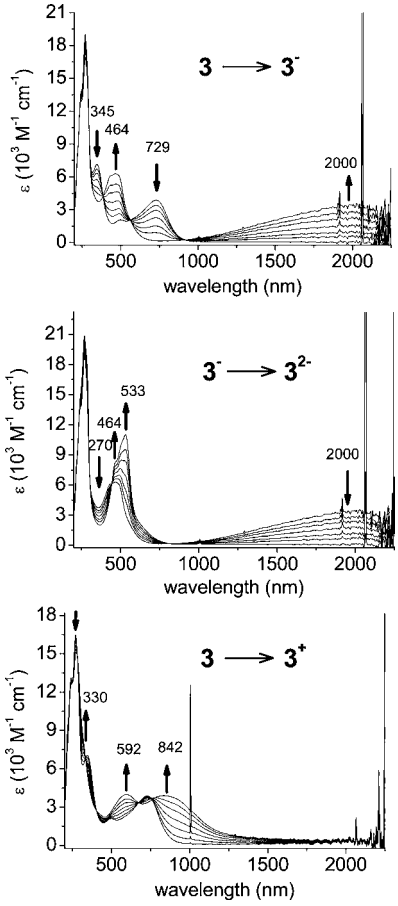

Figure 5. UV−vis−NIR spectroelectrochemical reduction and oxidation of **3** in CH_3CN/0.1 M Bu_4NPF_6 at 298 K.

The formation of cations $\mathbf{3}^+$ and $\mathbf{4}^+$ is accompanied by the emergence of two long-wavelength bands at about 820 and 595 nm (Table 4). An electronic description as mentioned above, a $Ru^{III}(\mu\text{-adc-O}^i\text{Pr}^{\bullet-})Ru^{III}$ configuration, would be compatible with such a nonmixed valent situation.

Regarding the question of potentially noninnocent behavior, the stepwise reduction via the intermediates $\mathbf{1}^-$−$\mathbf{4}^-$ is most revealing. In addition to the expected LMCT absorptions (π(adc-OR)→d, π(acac)→d) of Ru^{III} involving species around 800 nm and the MLCT transitions of Ru^{II} containing forms in the visible region of about 500 nm (Figure 5, Table 4), the most conspicuous feature of the spectroelectrochemical study of compounds **1**−**4** is the formation of fairly intense ($\varepsilon \approx 3000$ M^{-1} cm^{-1}) and broad ($\Delta\nu_{1/2} \approx 3000$ cm^{-1}) near-infrared absorption bands of the monoanions at about $\lambda_{max} \approx 2000$ nm ($\tilde{\nu}_{max} \approx 5000$ cm^{-1}; Table 5). Although not optimally suited for fiber optics technology with its preference for the 1500 nm region, electrochromic materials operating at about 2000 nm wavelength have recently received special attention.[45]

NIR bands of oligonuclear metal complexes with noninnocent bridging ligands can be assigned either to intervalence charge transfer (IVCT) transitions of a mixed-valent species or to intra-radical transitions of a homovalent alternative (**A**, **B** in Scheme 1).[1a]

Table 4. Absorption Values from UV-vis-NIR Spectroelectrochemistry[a]

compound	λ_{max}/nm ($\varepsilon/10^{-3}$ M^{-1} cm^{-1})
1	726 (2.3), 499 (1.3), 345 (4.8)
$\mathbf{1}^-$	1910 (2.8), 459 (4.0), 438 (4.0)
$\mathbf{1}^{2-}$	540 (6.4), 480 (sh)
2	734 (3.4), 494 (1.6), 346 (6.0)
$\mathbf{2}^-$	2000 (3.1), 465 (5.0), 436 (5.0)
$\mathbf{2}^{2-}$	540 (9.0), 472 (sh)
3	729 (3.9), 497 (2.1), 345 (7.1)
$\mathbf{3}^-$	2000 (3.5), 464 (6.3), 440 (sh)
$\mathbf{3}^{2-}$	533 (11.0), 464 (sh)
$\mathbf{3}^+$	842 (4.0), 592 (4.1)
4	721 (3.7), 499 (2.3), 345 (7.7)
$\mathbf{4}^-$	1932 (4.4), 463 (6.8), 435 (6.7)
$\mathbf{4}^{2-}$	534 (11.7), 472 (sh)
$\mathbf{4}^+$	800 (3.7), 599 (4.8)

[a]From spectroelectrochemistry in an OTTLE cell in CH_3CN/0.1 M Bu_4NPF_6 at 298 K.

Table 5. Intervalence Charge Transfer Data for Anions

compound	λ_{IVCT}/nm ($\varepsilon/10^{-3}$ M^{-1} cm^{-1})	$\Delta\nu_{1/2}$[a]/cm^{-1}
$\mathbf{1}^-$	1910 (2.76)	2850
$\mathbf{2}^-$	2000 (3.10)	3300
$\mathbf{3}^-$	2000 (3.46)	3300
$\mathbf{4}^-$	1932 (4.40)	2800

[a]Experimental bandwidths at half-height in cm^{-1}.

The EPR- and DFT-supported characterization of the monoanions as mixed-valent species invites a Hush analysis of the linewidths of the near-infrared bands (Table 5). The experimentally assessed line-widths at half height of about $\Delta\nu_{1/2} \approx 3000$ cm^{-1} lie somewhat higher than the numbers $\Delta\nu_{1/2}$(calc) ≈ 2100 cm^{-1} which were obtained from the formula $\Delta\nu_{1/2}$ (calc) = $(2310 \times \nu_{max})^{1/2}$ that holds for class II mixed-valent systems.[41] The $\Delta\nu_{1/2}$ values had to be estimated from the experimentally accessible shorter-wavelength sections of the spectral bands (Figure 5), and the long-wavelength limitation did not allow us to examine a possible asymmetric character of the bands. Neither the comproportionation constants of $K_c = 10^8$−10^{10} nor the intense near-infrared absorptions can thus unequivocally confirm a localized or delocalized valence situation for the species $\mathbf{1}^-$−$\mathbf{4}^-$. Class II/III borderline situations have been postulated, inter alia, for the Creutz−Taube ion.[45]

Calculation of the V_{AB} interaction parameter according to the equations summarized by Richardson and Taube[41a] yields values of about 1000 cm^{-1}, in between that of the strongly coupled Creutz−Taube ion (V_{AB} = 3200 cm^{-1}) and those of weakly coupled dicyanobenzene-bridged bis(pentaammino)-ruthenium(III,II) systems (V_{AB} < 400 cm^{-1}).[41c] In contrast to these acceptor-bridged cationic species, the donor bridged anions $\mathbf{1}^-$−$\mathbf{4}^-$ rely on a hole-transfer mechanism[7,41b,c] for valence exchange.

■ CONCLUSION

This paper describes neutral stereoisomeric diruthenium(III) species $[(acac)_2Ru(\mu\text{-adc-OR})Ru(acac)_2]$ with significant stereodependent antiferromagnetic spin−spin coupling. When negatively charged, the resulting EPR silent monoanions retain the innocently behaving bridging ligand dianions and the

dx.doi.org/10.1021/ic300809w | Inorg. Chem. 2012, 51, 9273−9281

diruthenium(III,II) mixed valency leads to intense, broad IVCT absorptions around 2000 nm. The effects from the ancillary ligands (π-donating acac$^-$ vs π-accepting bpy) and from the bridge (substituent effects of R, accepting carbonyl vs less accepting imine) are responsible for the differences in the electronic structures, varying between mixed-valent species $Ru^{III}(\mu\text{-}L^{2-})Ru^{II}$ (**B**) and the radical bridged alternative $Ru^{II}(\mu\text{-}L^{\bullet-})Ru^{II}$ (**A**).

The redox series $[(acac)_2Ru(\mu\text{-adc-OR})Ru(acac)_2]^n$, n = 0,−,2− and especially the monoanionic intermediate fill a gap between the series $[(bpy)_2Ru(\mu\text{-adc-R})Ru(bpy)_2]^n$, n = 4+,3+,2+ (**5** in Scheme 1), with accepting bpy instead of donating acac$^-$ as ancillary ligands on one side,[7] and in relation to the series $[(acac)_2Ru(\mu\text{-dih-R})Ru(acac)_2]^n$, n = 0,−,2− with the all-N containing dih-R bridge (**6** in Scheme 1) instead of adc-R.[8] The most sensitive intermediates with their alternative between the $Ru^{III}(L^{2-})Ru^{II}$ mixed-valence formulation (**B**) (Scheme 1) and the radical ion alternative $Ru^{II}(L^{\bullet-})Ru^{II}$ (**A**) show remarkable but understandable effects:

The easier reduction of the C═O versus C═NH bridge (electronegativity) results in a preference of $[(acac)_2Ru(\mu\text{-adc-OR})Ru(acac)_2]^-$ for **B** (with 2e-reduced bridge) and of $[(acac)_2Ru(\mu\text{-dih-R})Ru(acac)_2]^-$ for **A** (1e-reduced bridge), as shown here and in ref 8. On the other hand, the stabilization of Ru^{II} by bpy and of Ru^{III} by acac$^-$ results in a substituent dependent ambivalent situation (**B** or the diruthenium(II) form **A**) for $[(bpy)_2Ru(\mu\text{-adc-R})Ru(bpy)_2]^{3+}$, whereas systems $[(acac)_2Ru(\mu\text{-adc-OR})Ru(acac)_2]^-$ as introduced here clearly prefer the mixed-valent situation **B** with predominantly oxidized metals.

■ ASSOCIATED CONTENT

Ⓢ Supporting Information

CIF and CIFcheck data for **3** × H_2O. Figures from studies of magnetism: Hysteresis loops for complex **3** (Figure S1); magnetization versus magnetic field cycles (Figures S2, S4); ZFC and FC temperature dependence of the molar magnetic susceptibility of **3** (Figure S3); temperature dependence of magnetic susceptibility and magnetic moment for complex **4** (Figure S5). This material is available free of charge via the Internet at http://pubs.acs.org.

■ AUTHOR INFORMATION

Corresponding Author

*E-mail: kaim@iac.uni-stuttgart.de (W.K.).

Notes

The authors declare no competing financial interest.

[⊥]Deceased, May 28, 2011.

■ ACKNOWLEDGMENTS

Financial support received from the DAAD, FCI, and DFG (Germany), the Spanish MICINN (CTQ 2008-00920), C.M. (S-0505-MAT-0303), and UCM (921073), the Czech Republic (Grant LD11086), and the Department of Science and Technology, New Delhi, India is gratefully acknowledged.

■ REFERENCES

(1) (a) Kaim, W. *Coord. Chem. Rev.* **2011**, *255*, 2503 , and literature cited. (b) Yao, C.-J.; Zhong, Y.-W.; Nie, H.-J.; Abruña, H. D.; Yao, J. *J. Am. Chem. Soc.* **2011**, *133*, 20720.

(2) (a) Qian, G.; Wang, Z. Y. *Chem.—Asian J.* **2010**, *5*, 1006. (b) LeClair, G.; Wang, Z. Y. *J. Solid State Electrochem.* **2009**, *13*, 365. (c) Ward, M. D. *J. Solid State Electrochem.* **2005**, *9*, 778.

(3) Kao, C. K. *Sand from centuries past; Send future voices fast*, Nobel Prize lecture, December 8th, 2009.

(4) (a) Qi, Y.; Desjardins, P.; Wang, Z. Y. *J. Opt. A: Pure Appl. Opt.* **2002**, *4*, S273. (b) Qi, Y.; Wang, Z. Y. *Macromolecules* **2003**, *36*, 3146. (c) Qi, Y.-H.; Desjardins, P.; Birau, M.; Wu, X.-G.; Wang, Z.-Y. *Chin. J. Polym. Sci.* **2003**, *21*, 147.

(5) (a) Qi, Y. H.; Desjardins, P.; Meng, X. S.; Wang, Z. Y. *Opt. Mater.* **2002**, *21*, 255. (b) Wang, Z. Y.; Zhang, J.; Wu, X.; Birau, M.; Yu, G.; Yu, H.; Qi, Y.; Desjardin, P.; Meng, X.; Gao, J. P.; Todd, E.; Song, N.; Bai, Y.; Beaudin, A. M. R.; LeClair, G. *Pure Appl. Chem.* **2004**, *76*, 1435.

(6) (a) Wang, S.; Li, X.; Xun, S.; Wan, X.; Wang, Z. Y. *Macromolecules* **2006**, *39*, 7502. (b) Zhang, J.; Wu, X.; Yu, H.; Yan, D.; Wang, Z. *Chin. Sci. Bull.* **2005**, *50*, 2688. (c) Xun, S.; LeClair, G.; Zhang, J.; Chen, X.; Gao, J. P.; Wang, Z. Y. *Org. Lett.* **2006**, *8*, 1697. (d) Li, D.; Wang, Z. Y.; Ma, D. *Chem. Commun.* **2009**, 1529.

(7) (a) Kasack, V.; Kaim, W.; Binder, H.; Jordanov, J.; Roth, E. *Inorg. Chem.* **1995**, *34*, 1924. (b) Jana, R.; Sarkar, B.; Bubrin, D.; Fiedler, J.; Kaim, W. *Inorg. Chem. Commun.* **2010**, *13*, 1160.

(8) Maji, S.; Sarkar, B.; Patra, S.; Fiedler, J.; Mobin, S. M.; Puranik, V. G.; Kaim, W.; Lahiri, G. K. *Inorg. Chem.* **2006**, *45*, 1316.

(9) Kaim, W. *Coord. Chem. Rev.* **2001**, *219*−*221*, 463.

(10) Jørgensen, C. K. *Coord. Chem. Rev.* **1966**, *1*, 164.

(11) Ward, M. D.; McCleverty, J. A. *J. Chem. Soc., Dalton Trans.* **2002**, 275.

(12) Agarwala, H.; Scherer, T.; Maji, S.; Mondal, T. K.; Mobin, S. M.; Fiedler, J.; Urbanos, F. A.; Jiménez-Aparicio, R.; Kaim, W.; Lahiri, G. K. *Chem.—Eur. J.* **2012**, *18*, 5667.

(13) Knödler, A.; Fiedler, J.; Kaim, W. *Polyhedron* **2004**, *23*, 701.

(14) But, T. Y. S.; Toy, P. H. *Chem.—Asian J.* **2007**, *2*, 1340.

(15) (a) Ernst, S.; Kasack, V.; W. Kaim, W. *Inorg. Chem.* **1988**, *27*, 1146. (b) Keene, F. R. *Chem. Soc. Rev.* **1998**, *27*, 185.

(16) (a) Dzik, W. I.; van der Vlugt, J. I.; Reek, J. N. H.; de Bruin, B. *Angew. Chem.* **2011**, *123*, 3416; *Angew. Chem., Int. Ed.* **2011**, *50*, 3356. (b) de Bruin, B. *Eur. J. Inorg. Chem.* **2012**, 340.

(17) (a) Kaim, W. *Inorg. Chem.* **2012**, *50*, 9752. (b) Kaim, W. *Eur. J. Inorg. Chem.* **2012**, 343.

(18) Kobayashi, T.; Nishina, Y.; Shimizu, K. G.; Sato, G. P. *Chem. Lett.* **1988**, 1137.

(19) Krejcik, M.; Danek, M.; Hartl, F. *J. Electroanal. Chem.* **1991**, *317*, 179.

(20) Kaim, W.; Ernst, S.; Kasack, V. *J. Am. Chem. Soc.* **1990**, *112*, 173.

(21) Sheldrick, G. M. *SHELX* ∼ *S97*; University of Göttingen: Göttingen, Germany, 1997.

(22) Frisch, M. J.; Trucks, G. W.; Schlegel, H. B.; Scuseria, G. E.; Robb, M. A.; Cheeseman, J. R.; Scalmani, G.; Barone, V.; Mennucci, B.; Petersson, G. A.; Nakatsuji, H.; Caricato, M.; Li, X.; Hratchian, H. P.; Izmaylov, A. F.; Bloino, J.; Zheng, G.; Sonnenberg, J. L.; Hada, M.; Ehara, M.; Toyota, K.; Fukuda, R.; Hasegawa, J.; Ishida, M.; Nakajima, T.; Honda, Y.; Kitao, O.; Nakai, H.; Vreven, T.; Montgomery, J. A., Jr.; Peralta, J. E.; Ogliaro, F.; Bearpark, M.; Heyd, J. J.; Brothers, E.; Kudin, K. N.; Staroverov, V. N.; Kobayashi, R.; Normand, J.; Raghavachari, K.; Rendell, A.; Burant, J. C.; Iyengar, S. S.; Tomasi, J.; Cossi, M.; Rega, N.; Millam, J. M.; Klene, M.; Knox, J. E.; Cross, J. B.; Bakken, V.; Adamo, C.; Jaramillo, J.; Gomperts, R.; Stratmann, R. E.; Yazyev, O.; Austin, A. J.; Cammi, R.; Pomelli, C.; Ochterski, J. W.; Martin, R. L.; Morokuma, K.; Zakrzewski, V. G.; Voth, G. A.; Salvador, P.; Dannenberg, J. J.; Dapprich, S.; Daniels, A. D.; Farkas, O.; Foresman, J. B.; Ortiz, J. V.; Cioslowski, J.; Fox, D. J. *Gaussian 09* , Revision B.01; Gaussian, Inc.: Wallingford, CT, 2009.

(23) (a) te Velde, G.; Bickelhaupt, F. M.; van Gisbergen, S. J. A.; Fonseca Guerra, C.; Baerends, E. J.; Snijders, J. G.; Ziegler, T. *J. Comput. Chem.* **2001**, *22*, 931. (b) *ADF2010.01*; SCM, Theoretical Chemistry, Vrije Universiteit: Amsterdam, The Netherlands, http://www.scm.com.

(24) (a) Perdew, J. P.; Burke, K.; Ernzerhof, M. *Phys. Rev. Lett.* **1996**, *77*, 3865. (b) Adamo, C.; Barone, V. *J. Chem. Phys.* **1999**, *110*, 6158.

(25) Krishnan, R.; Binkley, J. S.; Seeger, R.; Pople, J. A. *J. Chem. Phys.* **1980**, *72*, 650.

(26) Hehre, W. J.; Ditchfield, R.; Pople, J. A. *J. Chem. Phys.* **1972**, *56*, 2257.
(27) Andrae, D.; Häussermann, U.; Dolg, M.; Stoll, H.; Preuss, H. *Theor. Chim. Acta* **1990**, *77*, 123.
(28) Martin, J. M. L.; Sundermann, A. *J. Chem. Phys.* **2001**, *114*, 3408.
(29) (a) Neese, F. *J. Phys. Chem. Solids* **2004**, *65*, 781. (b) Noodleman, L. *J. Chem. Phys.* **1981**, *74*, 5737.
(30) Lahti, P. M.; Ichimura, A. S.; Sanborn, J. A. *J. Phys. Chem. A* **2001**, *105*, 251.
(31) Becke, A. D. *Phys. Rev. A* **1988**, *38*, 3098.
(32) Perdew, J. P.; Wang, Y. *Phys. Rev. B* **1992**, *45*, 13244.
(33) (a) Das, A.; Scherer, T.; Maji, S.; Mondal, T. K.; Mobin, S. M.; Urbanos, F. A.; Jiménez-Aparicio, R.; Kaim, W.; Lahiri, G. K. *Inorg. Chem.* **2011**, *50*, 7040. (b) See also: Pritchard, B.; Autschbach, J. *Inorg. Chem.* **2012**, *51*, 8340.
(34) (a) Zárate, X.; Schott, E.; Mac-Leod Carey, D.; Bustos, C.; Arratia-Pérez, R. *J. Mol. Struct.: THEOCHEM* **2010**, *957*, 126. (b) Das, A.; Scherer, T. M.; Mobin, S. M.; Kaim, W.; Lahiri, G. K. *Chem.—Eur. J.* **2012**, *18*, 11007. (c) Pestana, D. C.; Power, P. P. *Inorg. Chem.* **1991**, *30*, 528.
(35) (a) Shivakumar, M.; Pramanik, K.; Ghosh, P.; Chakravorty, A. *Inorg. Chem.* **1998**, *37*, 5968. (b) Pramanik, K.; Shivakumar, M.; Ghosh, P.; Chakravorty, A. *Inorg. Chem.* **2000**, *39*, 195.
(36) Muñiz, K.; Nieger, M. *Angew. Chem.* **2006**, *118*, 2363; *Angew. Chem., Int. Ed.* **2006**, *45*, 2305.
(37) Y. Tomiie, Y.; Koo, C. H.; Nitta, I. *Acta Crystallogr.* **1958**, *11*, 774.
(38) Berg, J. M.; Tymoczko, J. L.; Stryer, L. *Biochemistry*, 6th ed.; W. H. Freeman: New York, 2007; p 38.
(39) Kahn, O. *Molecular Magnetism*; VCH Publishers: New York, 1993.
(40) Das, D.; Sarkar, B.; Kumbhakar, D.; Mondal, T. K.; Mobin, S. M.; Fiedler, J.; Urbanos, F. A.; Jiménez-Aparicio, R.; Kaim, W.; Lahiri, G. K. *Chem.—Eur. J.* **2011**, *17*, 11030.
(41) (a) Richardson, D. E.; Taube, H. *J. Am. Chem. Soc.* **1983**, *105*, 40. (b) Kaim, W.; Lahiri, G. K. *Angew. Chem.* **2007**, *119*, 1808; *Angew. Chem., Int. Ed.* **2007**, *46*, 1778. (c) Crutchley, R. J. *Adv. Inorg. Chem.* **1994**, *41*, 273.
(42) (a) Rieger, P. H. *Electron Spin Resonance*; The Royal Society of Chemistry: Cambridge, U.K., 2007. (b) Sarkar, B.; Patra, S.; Fiedler, J.; Sunoj, R. B.; Janardanan, D.; Lahiri, G. K.; Kaim, W. *J. Am. Chem. Soc.* **2008**, *130*, 3532. (c) Sarkar, B.; Patra, S.; Fiedler, J.; Sunoj, R.; Janardanan, D.; Mobin, S. M.; Niemeyer, M.; Lahiri, G. K.; Kaim, W. *Angew. Chem.* **2005**, *117*, 5800; *Angew. Chem., Int. Ed.* **2005**, *44*, 5655.
(43) Kaim, W.; Kasack, V. *Inorg. Chem.* **1990**, *29*, 4696.
(44) (a) Chaudhuri, P.; Verdani, C. N.; Bill, E.; Bothe, E.; Weyhermüller, T.; Wieghardt, K. *J. Am. Chem. Soc.* **2001**, *123*, 2213. (b) Ye, S.; Sarkar, B.; Lissner, F.; Schleid, Th.; van Slageren, J.; Fiedler, J.; Kaim, W. *Angew. Chem.* **2005**, *117*, 2140; *Angew. Chem., Int. Ed.* **2005**, *44*, 2103.
(45) Dinolfo, P. H.; Williams, R. D.; Hupp, J. T. *Chem. Phys.* **2005**, *319*, 28.